SPRING AND ASYMPTOTIC BOUNDARY CONDITION MODELS FOR STUDY OF SCATTERING BY THIN CYLINDRICAL INTERPHASES

W. Huang and S.I. Rokhlin
The Ohio State University
Department of Welding Engineering
Columbus, Ohio 43210

INTRODUCTION

Specially designed fiber-matrix interphases are created in modern composites to improve fracture toughness, chemical compatibility and matching of thermal expansion coefficients between composite constituents [1, 2, 3]. Since the interphase transfers the load from matrix to fiber, the interphase elastic moduli, thickness and the quality of bonding with the surrounding fiber and matrix are essential in determining composite mechanical performance. Such interphase conditions can be sensed by ultrasonic waves due to strong interphase effects on wave scattering from fibers. However the interphase properties (elastic modulus and thickness) are in-situ parameters and are often difficult to define. One way to get around this is to introduce simplified boundary condition (B.C.) models to describe the displacement and stress fields across the interphase directly. In this paper we will address this problem with emphasis on spring and asymptotic B.C. models as a representation of a thin fiber-matrix interphase when studying wave scattering from fibers.

Although much work has been done for elastic wave scattering from a cylindrical inclusion in a solid [4, 5, 6, 7, 8, 9], almost all previous studies address scattering of an elastic wave on a solid cylinder perfectly bonded to the solid matrix. In our own work [10, 11] scattering from multiphase fibers with focus on the effect of fiber-matrix interphasial regions has been reported. A transfer matrix formalism was developed in [11] to simplify the treatment of the multilayered cylindrical system. Here we will give an alternative approach to obtain the transfer matrix, which is more convenient for deriving different B.C. models to represent a thin fiber-matrix interphase.

TRANSFER MATRIX SOLUTION OF SCATTERING FROM A MULTILAYERED FIBER IN SOLID

The elastic wave solutions in a cylindrical system have the following general form:

$$\varphi = \sum_{n=-\infty}^{\infty} [A_n J_n(k_l r) + C_n N_n(k_l r)] \exp(in\theta), \tag{1}$$

$$\psi_z = \sum_{n=-\infty}^{\infty} [B_n J_n(k_t r) + D_n N_n(k_t^j r)] \exp(in\theta), \tag{2}$$

where φ is the scalar potential and ψ_z is the z-component of vector potential; k_l and k_t are the wave numbers of the longitudinal and transverse modes, and $J_n(\cdot)$ and $N_n(\cdot)$ are the nth order Bessel and Neumann functions. The time-dependent factor $e^{-i\omega t}$ is omitted throughout. For a cylindrical system (see Fig. 1) whose properties have

Review of Progress in Quantitative Nondestructive Evaluation, Vol. 15
Edited by D.O. Thompson and D.E. Chimenti, Plenum Press, New York, 1996

only radial dependence, one can obtain a governing matrix differential equation for the elastic field by combining Newton's second law, the wave equation and Hooke's law as

$$\frac{\partial \vec{U}_n(r)}{\partial r} = \mathbf{t_n(r)}\vec{U}_n(r) \tag{3}$$

where $\vec{U}_n(r)$ denotes the displacement and stress vector $(u_r, u_\theta, \sigma_{rr}, \sigma_{r\theta})_n^T$, and $\mathbf{t_n(r)}$ is the characteristic matrix of the elastic field at position r:

$$\mathbf{t_n(r)} = \begin{pmatrix} -\frac{\lambda}{r(\lambda+2\mu)} & -\frac{in\lambda}{r(\lambda+2\mu)} & \frac{1}{\lambda+2\mu} & 0 \\ -\frac{in}{r} & \frac{1}{r} & 0 & \frac{1}{\mu} \\ \frac{4\mu(\lambda+\mu)}{r^2(\lambda+2\mu)} - \rho\omega^2 & \frac{4in\mu(\lambda+\mu)}{r^2(\lambda+2\mu)} & -\frac{2\mu}{r(\lambda+2\mu)} & -\frac{in}{r} \\ -\frac{4in\mu(\lambda+\mu)}{r^2(\lambda+2\mu)} & \frac{4n^2\mu(\lambda+\mu)}{r^2(\lambda+2\mu)} - \rho\omega^2 & -\frac{in\lambda}{r(\lambda+2\mu)} & -\frac{2}{r} \end{pmatrix}. \tag{4}$$

Here λ, μ are Lamé constants and ρ is the density.

Equation (3) has a well-known exponential solution:

$$\vec{U}_n(r+\delta r) = \exp\{\int_r^{r+\delta r} \mathbf{t_n(r)}dr\}\vec{U}_n(r). \tag{5}$$

Applying this solution to scattering from a multilayered fiber in a solid (Fig. 1), the transfer matrix for an intermediate layer ($r_{j-1} \le r \le r_j$) can be found as

$$\mathbf{T_n^j} = \exp\{\int_{r_{j-1}}^{r_j} \mathbf{t_n^j(r)}dr\} = \mathbf{I} + \int_{r_{j-1}}^{r_j} \mathbf{t_n^j(r)}dr + \int_{r_{j-1}}^{r_j} \mathbf{t_n^j(r)}dr \int_{r_{j-1}}^{r} \mathbf{t_n^j}(\tau)d\tau + \cdots \tag{6}$$

Using the transfer matrix for each intermediate cylindrical layer, the stresses and displacements on the outer boundary of the multilayered cylinder ($r = r_{N-1}$) can be directly related to those in the fiber core ($r = r_1$) as

$$(u_r^N, u_\theta^N, \sigma_{rr}^N, \sigma_{r\theta}^N)_n^T|_{r=r_{N-1}} = \mathbf{T_n^{N-1}T_n^{N-2}}\cdots\mathbf{T_n^2}\cdot(u_r^1, u_\theta^1, \sigma_{rr}^1, \sigma_{r\theta}^1)_n^T|_{r=r_1} \tag{7}$$

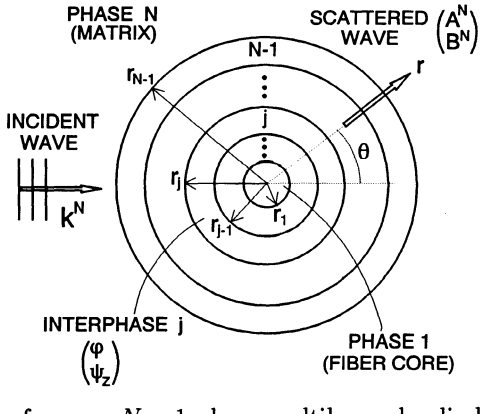

Figure 1. Scattering from an $N-1$ phase multilayered cylinder in a solid matrix. k^N is the incident wave number in the matrix material (phase N).

The solution for the scattering coefficients A_n^N and B_n^N (see Fig. 1) are found by solving the 4×4 B.C. equation (7) (for details see [11]). The scattering cross-section, which is defined as the total power scattered per unit length divided by the incident wave intensity (power per unit area), is found as [6]:

$$Q_l = \frac{1}{k_{(l,t)}^N r_{N-1}} \sum_{n=-\infty}^{\infty} |A_n^N|^2, \quad Q_t = \frac{1}{k_{(l,t)}^N r_{N-1}} \sum_{n=-\infty}^{\infty} |B_n^N|^2, \tag{8}$$

where Q_l and Q_t are the non-dimensional scattering cross-sections, normalized by the geometric scattering limit $4r_{N-1}$ (r_{N-1} is the fiber radius including the outermost interphase). $k_{(l,t)}^N$ is the incident wave number for the longitudinal or transverse mode in the matrix material (phase N). For transverse isotropic media, one need only replace λ and μ in equations (4) by $C_{rr} - 2G_t$ and G_t respectively, where C_{rr} is the radial modulus and G_t is the transverse shear modulus.

REPRESENTATION OF A THIN FIBER-MATRIX INTERPHASE BY APPROXIMATE B.C. MODELS

As shown previously we can apply the transfer matrix (6) to describe exactly the scattering from the fiber-matrix interphase with thickness $h = r_i - r_f$, where r_f and r_i are the radii of the interphase inner and outer boundary. When the fiber-matrix interphase is thin, i.e. $h \ll r_f$ and $k_{l,t}^i h \ll 1$, one can take the first order approximation in h of asymptotic expansion (6):

$$\vec{U}_n(r = r_i) = \mathbf{T_n^i} \vec{U}_n(r = r_f), \quad \text{where } \mathbf{T_n^i} \approx \mathbf{I} + h\mathbf{t_n^i}(\mathbf{r_f}), \tag{9}$$

where $\mathbf{T_n^i}$ is the first order transfer matrix for the interphase and equation (9) is the first order asymptotic B.C.

One may also define the second order asymptotic B.C. as in case of plane interphase [13, 14] by applying the finite difference approximation to the matrix differential equation (3)

$$\frac{\vec{U}_n(r = r_i) - \vec{U}_n(r = r_f)}{h} = \mathbf{t_n}(\mathbf{r} = \bar{\mathbf{r}}) \frac{\vec{U}_n(r = r_i) + \vec{U}_n(r = r_f)}{2}, \quad \bar{r} = \frac{r_f + r_i}{2}. \tag{10}$$

The second order B.C. (10) can be rewritten in the transfer matrix format as:

$$\vec{U}_n(r = r_i) = [\mathbf{I} - \frac{h}{2}\mathbf{t_n^i}(\bar{\mathbf{r}})]^{-1} [\mathbf{I} + \frac{h}{2}\mathbf{t_n^i}(\bar{\mathbf{r}})] \vec{U}_n(r = r_f). \tag{11}$$

It is reasonable to simply the B.C. across the interphase further by a spring model. This model has been used to describe the static elastic field on the fiber-matrix interface in composites [15, 16]. In their approach, an imperfect interface with the spring B.C. is taken where the springs are considered on an infinitely thin fiber-matrix boundary. Here we consider the spring B.C. in a different form to preserve the system geometry by applying the spring B.C. across the interphase gap instead of filling the gap by fiber or matrix materials. The advantage of using spring B.C. in this way will be discussed in the next section. If one keeps in the matrix (4) the spring stiffnesses terms, one obtains the spring B.C. as:

$$\begin{pmatrix} u_r \\ u_\theta \\ \sigma_{rr} \\ \sigma_{r\theta} \end{pmatrix}_n^{r=r_i} = \begin{pmatrix} 1 & 0 & \frac{h}{\lambda^i + 2\mu^i} & 0 \\ 0 & 1 & 0 & \frac{h}{\mu^i} \\ 0 & 0 & 1 & 0 \\ 0 & 0 & 0 & 1 \end{pmatrix} \begin{pmatrix} u_r \\ u_\theta \\ \sigma_{rr} \\ \sigma_{r\theta} \end{pmatrix}_n^{r=r_f}, \tag{12}$$

i.e.

$$\sigma_{rr}^m|_{r=r_i} = \sigma_{rr}^f|_{r=r_f} = K_n(u_r^m|_{r=r_i} - u_r^f|_{r=r_f}), \sigma_{r\theta}^m|_{r=r_i} = \sigma_{r\theta}^f|_{r=r_f} = K_t(u_\theta^m|_{r=r_i} - u_\theta^f|_{r=r_f}), \tag{13}$$

where $r = r_i$ is taken on the outer surface of the interphase and $r = r_f$ on the inner surface. The normal and shear spring stiffnesses are defined as $K_n = (\lambda^i + 2\mu^i)/h$ and $K_t = \mu^i/h$, where the superscript i indicates properties related to the interphase.

To demonstrate the applicability of different approximate B.C. models, we give numerical examples for longitudinal and shear wave scattering by a SiC fiber (SCS-6) in titanium alloy. The properties of each phase in the multiphase SCS-6 fiber are listed in Table 1, where E is Young's modulus, ν is Poisson's ratio, ρ is the density and r the radius of the boundary of that phase. The elastic properties of the carbon-rich interphase are taken equal to those of the carbon core; the interphase thickness is 3 μm. The scattering cross-section as a function of frequency calculated using different approximate B.C. models are shown in Fig. 2(a) for longitudinal wave incidence. In the figure the top axis is frequency in MHz, and the bottom axis is the nondimensional wave number $k_l^m r_i$ or $k_l^i h$. The second order solution (coarse dashed lines) is almost indistinguishable from the exact (solid lines). The spring (fine dashed lines) and first order (crosses) B.C. models also give good predictions at this interphase thickness and stiffness for low frequencies, especially for $k_l^m r_i < 4$ or $k_l^i h < 0.15$.

The difference between different approximations is more clearly seen with the increase of the interphase thickness to fiber radius ratio h/r_f. Fig. 2(b) shows the calculated scattering cross-sections versus h/r_f for shear wave incidence at frequency = 13 MHz ($k_t^i h = 0.08$). The fiber radius $r_f = 68\mu$m is kept constant. One sees from the figure that all B.C. models give good results for $h/r_f < 0.05$. For greater interphase thickness, the second order B.C. is good until $h/r_f = 0.2$, while the spring and first order B.C. models begin to deviate from the exact solution.

To demonstrate the quality of approximations by different B.C. for interphase layers with different stiffnesses we calculated the scattering cross-section versus interphase stiffnesses. In the calculations the interphase Young's modulus is varied while the interphase thickness, density and Poisson's ratio are kept constant. The results are shown in Fig. 3 for incident longitudinal wave at frequency $f = 13$ MHz and interphase thickness $h = 3\mu$m. In the figure, the horizontal axis is the interphase Young's modulus in log scale, and $E^m = 122$ GPa and $E^f = 415$ Gpa are the Young's moduli for the matrix and fiber shell respectively. One sees from the figure that the spring B.C. model give good predictions up to interphase stiffness equaling that of the fiber, while the first and second order asymptotic B.C. continue to give good results for much stiffer interphases.

It is interesting to discuss the limiting cases presented in Fig. 3. When the interphase Young's modulus is extremely small, the fiber with the interphase acts like a debonded fiber or a cylindrical cavity with radius that of the outer interphase boundary r_i. All the approximate B.C. models give the correct limit. For example, for the spring B.C. model, since K_n and K_t approach zero in this case, the spring B.C. (13) simplifies to

$$\sigma_{rr}^m|_{r=r_i} = \sigma_{r\theta}^m|_{r=r_i} = 0. \tag{14}$$

On the other hand, when the interphase Young's modulus is extremely high, the fiber with the interphase acts like a rigid cylinder with radius r_i, i.e. the B.C. should be

$$u_r^m|_{r=r_i} = u_\theta^m|_{r=r_i} = 0. \tag{15}$$

However, neither of the approximate B.C. models gives the correct limit. For the spring B.C. model, the B.C. reduce to welded B.C. across the interphase gap for the rigid interphase. Specifically, since K_n and K_t approach infinity, the spring B.C. (13) simplifies to

$$u_r^m|_{r=r_i} = u_r^f|_{r=r_f},\ \ u_\theta^m|_{r=r_i} = u_\theta^f|_{r=r_f},\ \ \sigma_{rr}^m|_{r=r_i} = \sigma_{rr}^f|_{r=r_f},\ \ \sigma_{r\theta}^m|_{r=r_i} = \sigma_{r\theta}^f|_{r=r_f}. \tag{16}$$

The discrepancy between the resulting B.C. for the rigid interphase (15) and rigid springs (16) explains the large deviation of the spring approximation for very high interphase stiffness as shown in Fig. 3. In summary the spring B.C. model is sufficient for a thin fiber-matrix interphase ($h/r_f < 0.05, k_{l,t}^i \ll 1$) which is softer than the fiber.

Table 1. Properties of each phase of the SCS-6 fiber and titanium alloy matrix.

Phase	E (GPa)	ν	λ (GPa)	μ (GPa)	ρ (g/cc)	r (μm)
core (carbon)	41	0.25	16	16	1.7	18
shell (SiC)	415	0.17	91	177	3.2	68
interphase	41	0.25	16	16	1.7	71
matrix (Ti)	122	0.35	103	45	5.4	

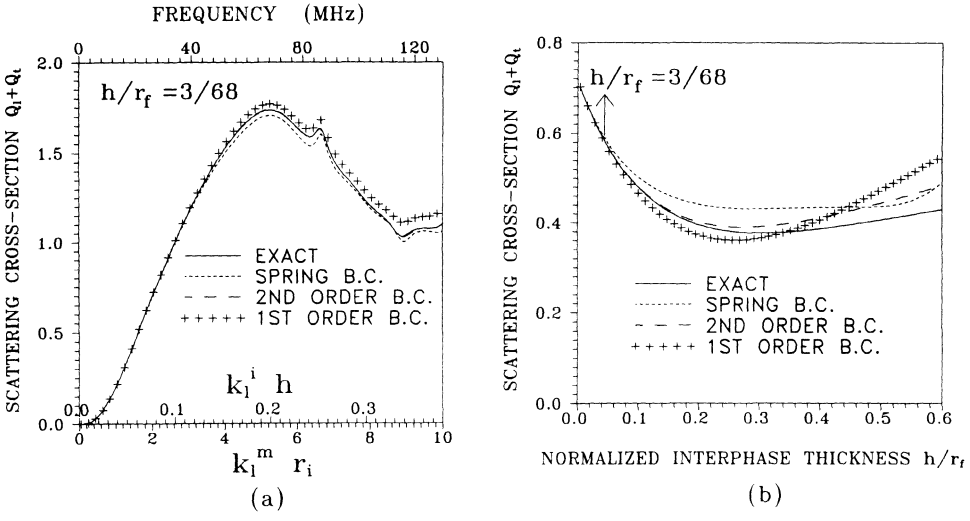

Figure 2. Scattering cross-sections calculated using different B.C. models. (a) Results versus frequency and wave number for longitudinal wave incidence ($h = 3$ μm). (b) Results versus interphase thickness h/r_f for shear wave incidence ($f = 13$ MHz).

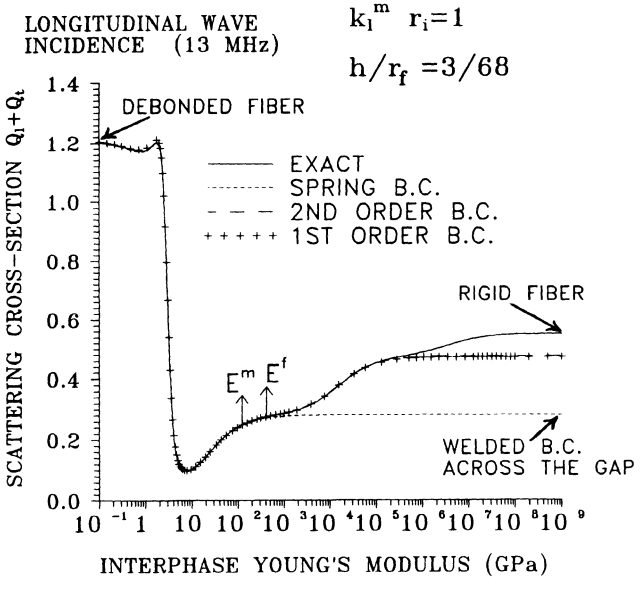

Figure 3. Scattering cross-sections versus interphase stiffnesses calculated using different B.C. models for longitudinal wave incidence ($f = 13$ MHz and $h = 3$ μm).

Another interesting observation from Fig. 3 is a minimum of the scattering cross-section. The minimum is explained by matching of impedances between matrix and the effective fiber formed by the actual fiber and the interphase. The decrease of the effective fiber impedance to that of the matrix and further results in a sharp increase in the scattering cross-section, reaching in the limit the scattering level from a cylindrical cavity for zero interphase moduli (disbond) [10, 11].

DISCUSSION OF SPRING B.C. MODEL: SPRINGS ON INTERPHASE GAP VERSUS THOSE ON INTERFACE BOUNDARY WITH GAP FILLED BY EITHER MATRIX OR FIBER

By applying the spring B.C. across an interphase gap we have kept the geometry of the problem unchanged. The different approach is to fill the interphase gap with either fiber or matrix material. This point is illustrated in Fig. 4 which shows three different ways of applying the springs to replace a thin fiber-matrix interphase. The first, as we did above, is to keep the interphase gap as shown by Fig. 4(b) and to use springs across the gap as given by (13). In this case the displacements jump across the interphase gap from r_f to r_i, while the stresses on both sides of the gap are the same. The other two ways involve applying the spring B.C. to an interface $r = R$ with the gap filled by either matrix or fiber materials:

$$\sigma^m_{rr}|_{r=R} = \sigma^f_{rr}|_{r=R} = K_n\,(u^m_r|_{r=R} - u^f_r|_{r=R}),\quad \sigma^m_{r\theta}|_{r=R} = \sigma^f_{r\theta}|_{r=R} = K_t\,(u^m_\theta|_{r=R} - u^f_\theta|_{r=R}). \tag{17}$$

Physically, $R = r_f$ implies that the interphase gap is filled by matrix as shown by Fig. 4(c), while $R = r_i$ corresponds to the case when the gap is filled by fiber as shown by Fig. 4(d). One sees from equation (17) that the displacements jump on the interface boundary $r = R$, while the stresses on this interface boundary are continuous.

Fig. 5 shows the calculated scattering cross-sections for an incident longitudinal wave versus (a) the nondimensional wave number and (b) interphase thickness to fiber radius ratio h/r_f. One sees from the figure that the spring B.C model (13) with interphase gap (the fine dashed line) gives the best results, while those (17) with gap filled by either matrix (crosses) or fiber (coarse dashed lines) material may deviate considerably from the exact even at low frequencies or small thicknesses. In general the spring B.C. model with gap filled by fiber material gives better results than the model with gap filled by matrix material. Note that the latter model predicts a

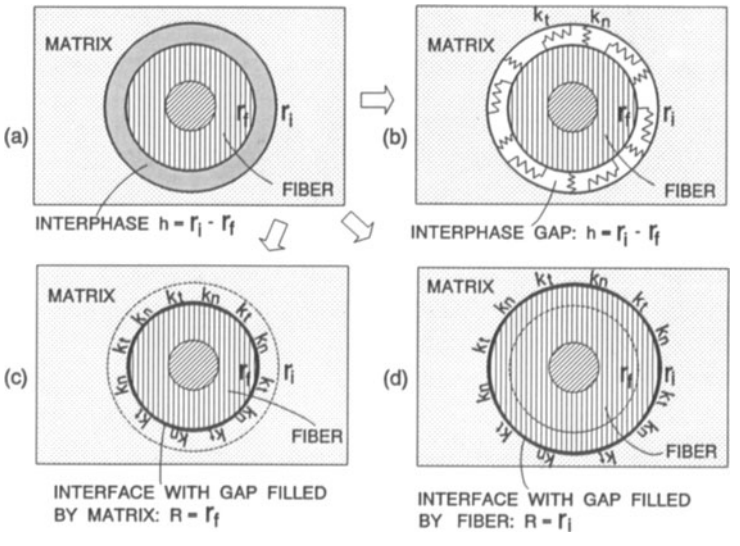

Figure 4. The exact interphase layer model and different spring B.C. models for a fiber-matrix interphase.

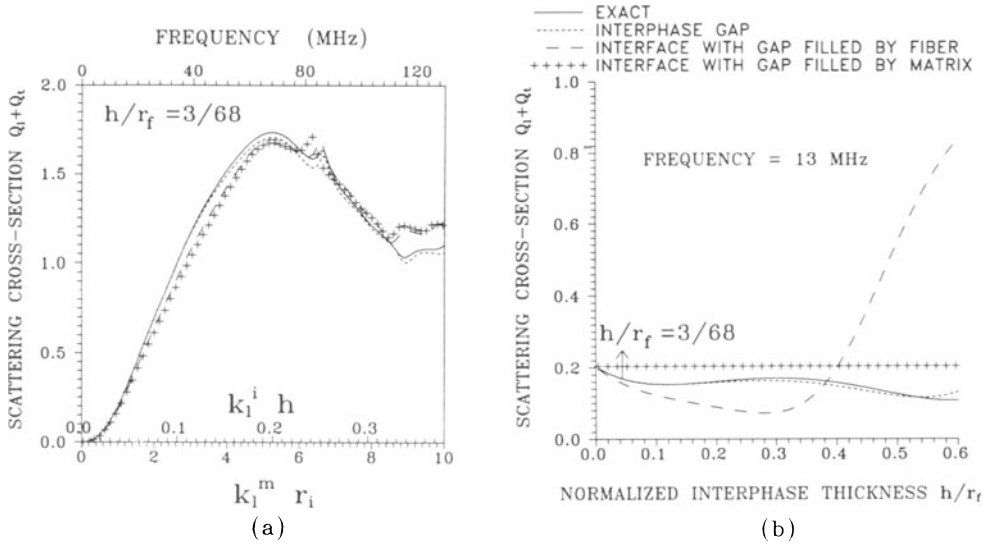

Figure 5. Scattering cross-sections calculated using different spring B.C. models. (a) Results vs frequency (wave number) for longitudinal wave incidence ($h = 3$ μm). (b) Results vs interphase thickness h/r_f for shear wave incidence ($f = 13$ MHz).

constant cross-section as interphase thickness increases since the fiber radius is constant. One can also apply the spring B.C. on the middle line of the gap by filling half of the gap by matrix and the other half by fiber. Simulations show that it does not provide any noticeable improvement than the model with gap filled by matrix.

Finally we calculated the scattering cross-section versus interphase stiffness using different spring B.C. models as in Fig. 3. The results are shown in Fig. 6 for longitudinal wave incidence at $f = 13$ MHz and h=3 μm. One sees from the figure that the spring B.C. model with gap filled by matrix gives totally unacceptable results in the scattering cross-section transition region to the limit of debonded fiber. The spring B.C. model with interphase gap gives good approximation for interphase stiffness below that of the fiber. The spring B.C. model with gap filled by fiber material gives acceptable results for less stiff interphases. Note that due to the difference in matrix and interphase densities and Poisson's ratios (see Table 1) the spring B.C. model with gap filled by matrix does not give satisfactory results even when the interphase Young's modulus equals that of the matrix.

We can interpret the results in Fig. 6 by examining the limits for very compliant and stiff interphases. First for an extremely compliant interphase the spring B.C. models with gap and with gap filled by fiber material yields the same free stress B.C. (14) (it provides the correct radius r_i of the cylindrical cavity). However the spring B.C. model with gap filled by matrix reduces to a cavity of a smaller radius of fiber (r_f). When the interphase Young's modulus is extremely high, none of the spring B.C. models give the rigid B.C. on the outer boundary of the interphase; instead they give welded B.C. across the gap or on the interface with gap filled by fiber or matrix.

CONCLUSIONS

We have applied a transfer matrix approach for analysis of wave scattering from a multilayered cylinder in a solid. The first and second order asymptotic B.C are derived

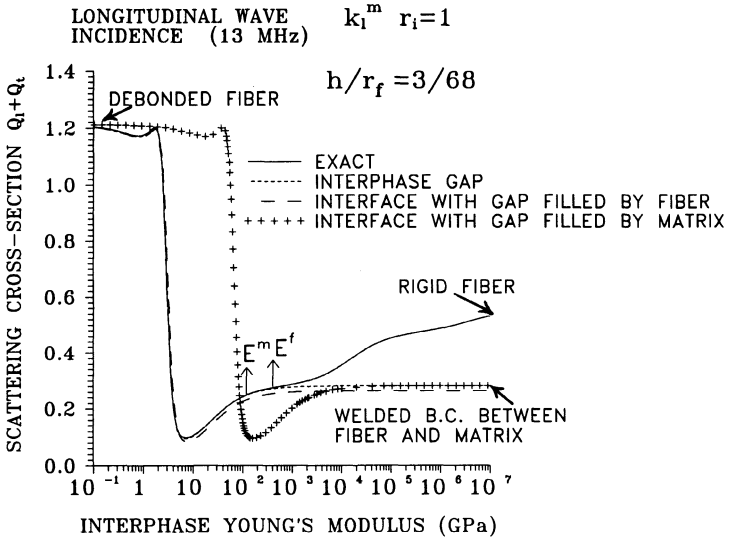

Figure 6. Scattering cross-sections vs interphase stiffnesses calculated using different spring B.C. models for longitudinal wave incidence (f = 13 MHz and h = 3 μm).

to replace a thin fiber-matrix interphase by asymptotically expanding the transfer matrix for the interphase. Different forms of spring B.C. models for the thin fiber-matrix interphase with interphase gap and with gap filled by matrix or fiber material are also studied. Since the interphase thickness may not be known exactly, there is an advantage in using the spring B.C. on a boundary between matrix and fiber by eliminating the gap and filling it with matrix material (usually the fiber diameter is known). In this case only two parameters K_n and K_t are needed to describe the mechanical contact across the interphase. Unfortunately when the gap is filled by matrix significant error may be introduced as has been shown by the above examples. Numerical analyses show that although the second order asymptotic B.C give the best overall results, the spring approximation with springs connecting the interphase gap is good for a thin ($h/r_f < 0.05, k_{l,t}^i h \ll 1$) interphase which is softer than the fiber. Alternatively the spring B.C. model with gap filled with fiber material may also be used with satisfactory results.

REFERENCES

1. A.G. Evans and D.B. Marshall, Mat. Res. Soc. Symp. Proc. 120, 213 (1988).
2. W.W. Wright, Compos. Polym. 3, 360 (1990).
3. A.K. Misra, in *HITEMP REVIEW-1991*, NASA CP-10082, 15-1 (1991).
4. R.M. White, J. Acous. Soc. Am. 30, 771 (1958).
5. V.V. Tyutekin, J. Sov. Phys. Acous. 5(1), 105 (1959).
6. Y.H. Pao and C.C. Mow, *Diffraction of Elastic Waves and Dynamic Stress Concentrations*, (Crane, Russack, New York, 1973).
7. D.J. Jain and R.P. Kanwal, J. Appl. Phys. 50, 4067 (1979).
8. P. Beattie, R.C. Chivers and L.W. Anson, J. Acous. Soc. Am. 94, 3421 (1993).
9. A.N. Sinclair and R.C. Addison, Jr., J. Acous. Soc. Am. 94, 1126 (1993).
10. W. Huang, S. Brisuda and S.I. Rokhlin, J. Acous. Soc. Am. 97, 807 (1995).
11. W. Huang, S.I. Rokhlin and Y.J. Wang, Ultrasonics 33, November (1995).
12. S.I. Rokhlin, and Y.J. Wang, J. Acoust. Soc. Am. 89, 503 (1991).
13. S.I. Rokhlin and W. Huang, J. Acoust. Soc. Am. 94, 3405 (1993).
14. W. Huang and S.I. Rokhlin, Geophy. J. Intern. 118, 285 (1994).
15. J. Aboudi, Composites Science and Technology, 28, 102 (1987).
16. Z. Hashin, Mechanics of Materials, 8, 333 (1990).